AAPS PharmSciTech, Vol. 19, No. 5, July 2018 (© 2018)
DOI: 10.1208/s12249-018-1013-4

Research Article

Bioactivity, Safety, and Efficacy of Amphotericin B Nanomicellar Aerosols Using Sodium Deoxycholate Sulfate as the Lipid Carrier

Faisal Usman,[1] Ruqaiya Khalil,[2] Zaheer Ul-Haq,[2] Titpawan Nakpheng,[1] and Teerapol Srichana[1,3,4]

Received 12 January 2018; accepted 3 April 2018; published online 24 April 2018

Abstract. We report nanomicelles of amphotericin B (AmB) using various molar ratios of AmB and sodium deoxycholate sulfate (SDCS) for inhalation with improved stability, solubility, bioactivity, and safety. The particle sizes of all aerosolized formulations are expressed as mass median aerodynamic diameter (0.9–1.6 μm), fine particle fraction (70.3–86.5%), and geometric standard deviation (1.4–2.1) which indicated their sizes are appropriate for use as an inhaler. *In vitro* cytotoxicity studies conducted using respiratory and kidney cell lines demonstrated that the marketed Fungizone® was toxic to macrophage and embryonic kidney cells and cell viability decreased from 96 to 48% and from 97 to 67%, respectively when the AmB equivalent concentration was increased from 1 to 16 μg/mL. However, AmB-SDCS formulations showed no evidence of toxicity even up to 8 μg/mL compared to Fungizone®. Minimum inhibitory and fungicidal concentrations were significantly reduced against *Cryptococcus neoformans*, and *Candida albicans.* Also, antileishmanial activity significantly improved for AmB-SDCS formulations. There was an evidence of phagocytosis of the AmB-SDCS formulation by alveolar macrophages NR 8383. Molecular modeling studies suggested the role of hydrogen bonding in stabilization of the AmB-SDCS complex. This study indicated that AmB-SDCS nanomicelles can be used to design a safe and cost-effective AmB for inhalation.

KEY WORDS: amphotericin B; sodium deoxycholate sulfate; toxicities; phagocytosis; molecular modeling.

INTRODUCTION

Invasive fungal infections have emerged as a major cause of morbidity and mortality particularly in immune-compromised patients (1,2). Currently, no optimum antifungal agent is available in clinical settings. Even though new antifungal agents like azoles and echinocandins possess low toxicity, they are associated with issues like erratic pharmacokinetics, limited spectrum of activity, drug interactions, and limited routes of administration (3,4).

Amphotericin B (AmB) is a broad-spectrum macrolide polyene antifungal drug, and it is the gold standard therapy against systemic and pulmonary fungal infections. However, it is insoluble in saline at a normal pH and when formulated with the surfactant sodium deoxycholate (SDC), it forms a colloidal dispersion of ribbon-like aggregates (5). Despite the clinical applications of AmB for over 50 years, it still exhibits excellent activity against a broad spectrum of fungi like *Candida* spp., *Aspergillus* spp., and filamentous fungi like Mucorales, *Cryptococcus*, histoplasmosis, blastomycosis, mucormycosis paracoccidioidomycosis, and coccidioidomycosis. Resistance is uncommon and tends to be species dependent (6). The physicochemical problem associated with AmB is the poor aqueous solubility which hinders its pulmonary formulation development. The severe toxicological issue is nephrotoxicity by binding with mammalian sterol of the cell membrane that subsequently leads to disruption of renal membrane physiology and results in ion leakage, reduced glomerular filtrate, loss of urine acidification, and urea excretion (7).

Liposomal and lipid complexes of AmB are less toxic and safe compared to Fungizone® with the added benefit of better aqueous solubility and the retention of *in vivo* antifungal efficacy (8). Although the liposomes has shown promising

[1] Drug Delivery System Excellence Centre, Department of Pharmaceutical Technology, Faculty of Pharmaceutical Sciences, Prince of Songkla University, Hat-Yai, Songkhla, 90112, Thailand.
[2] Computational Chemistry Unit, Dr. Panjwani Centre for Molecular Medicine and Drug Research, International Centre for Chemical and Biological Sciences, University of Karachi, Karachi, 75270, Pakistan.
[3] Nanotec-PSU Excellence Centre on Drug Delivery System, Department of Pharmaceutical Technology, Faculty of Pharmaceutical Sciences, Prince of Songkla University, Hat Yai, Songkhla, 90112, Thailand.
[4] To whom correspondence should be addressed. (e–mail: teerapol.s@psu.ac.th)

potential for nanoscale targeted drug delivery, their clinical applications are limited by lack of safety profiles (9). Also, higher doses are required to maintain blood therapeutic levels (10,11), which further result in accumulation of AmB-liposomes in the reticuloendothelial and phagocytic system leading to lysosomal storage disease. The marketed formulation of AmB, which is a physical complex of AmB and deoxycholic acid (Fungizone®), is a colloidal dispersion of AmB, and its therapeutic uses are limited owing to severe toxicity like acute infusion-related toxicities and chronic renal toxicity as well as dose-limited nephrotoxicity with increased risk of death (12–14). Furthermore, administration of nanoparticulate dosage forms is associated with plasma protein association that subsequently results in the modification of intended pharmacology and pharmacokinetics of the drug (15). There is continued interest for the development of a pulmonary dosage form of AmB with less or no renal toxicity.

This study presents sodium deoxycholate sulfate (SDCS) as a carrier for pulmonary delivery of AmB (Fig. 1). The formulations can be synthesized by single-step mixing which results in the formation of a loose aggregated micellar system. AmB-SDCS micellar formulations were found to be less toxic than the market formulation of Fungizone® against pulmonary and renal cells. Stabilization of the formulation complex was studied by molecular dynamics (MD) simulation. The AmB-SDCS formulation was studied for aerosol characteristics as well as the antifungal parameters (minimum inhibition concentration [MIC] and minimum fungicidal concentration [MCF]) as a nanomicelle system. Nebulized aerosol parameters were determined to assure the possibility of delivering the correct dosage form with the aid of a nebulizer. The formulation aimed for higher macrophagial uptake and improved antileishmanial activity against *Leishmania tropica (L. tropica).*

MATERIALS AND METHODS

AmB was generously donated by BioLab Co. Ltd. (Samustraprakan, Thailand). Sodium deoxycholate (SDC), sodium borohydride, and deoxycholic acid were obtained from Sigma-Aldrich (St. Louis, USA). Ethyl acetate, acetonitrile, hexane, chloroform, hydrochloric acid 37%, tetrahydrofuran, methanol, dichloromethane, and acetic acid were obtained from RCI Labscan Ltd. Bangkok, Thailand. Anhydrous sodium sulfate was purchased from Fischer Scientific, Leicestershire, UK. Sodium acetate hydrated was obtained from Ajax Finechem Pty Ltd., Auckland, New Zealand. Dimethyl sulphoxide (DMSO) was purchased from Riedel-de Haean, Germany. Polyamide membranes (pore size 0.22 μm) were purchased from Sartorius, Gottingen, Germany. All chemicals were of analytical grade and used without further purification.

Preparation of AmB-SDCS Nanoformulations

SDCS was synthesized using the method reported by Gangadhar et al., (2014) (16). AmB and SDCS nanoformulations were prepared using various concentrations of SDCS. Briefly, AmB (50 mg) and SDCS (26 mg) in a 1:1 M ratio were stirred in deionized water until completely dissolved. Approximately 2.7 mL of a 0.2 M sodium hydroxide solution was added slowly with continuous stirring at room temperature to obtain a clear yellowish solution. The pH of the solution was about 9.5 which was adjusted to 7.4 using phosphoric acid (0.2 M) for an *in situ* phosphate buffer. The final volume of the solution was made to 50 mL by adding approximately 25 mL deionized water. The solution was lyophilized and reconstituted in water for further studies. The solution took about 2 min for reconstitution with gentle shaking rendering clear solution**.** Using similar methods, various formulations were prepared using AmB and different molar ratios of SDCS (*i.e.*, 1:2 [50 and 52 mg], 1:3 [50 and 78 mg], 1:4 [50 and 104 mg], and 1:5 [50 and 130 mg]). The scheme of preparation of AmB-SDCS nanoformulations is shown in Fig. 2. A similar method was employed for preparation of the control formulation of AmB using sodium deoxycholate (SDC) in a 1:2 M ratio mimicking the commercially available formulation of Fungizone®. Freeze-dried formulations were stored at 4°C and protected from light.

Aerosol Properties of Reconstituted AmB-SDCS Nanoformulations

Lyophilized dry powder of various formulations of AmB-SDCS (*i.e.*, equivalent to 30 mg of AmB) was reconstituted with 6 mL of distilled water (5 mg/mL of AmB) for nebulization. The reconstituted solution (6 mL) was poured into a reservoir of a jet nebulizer (Westmed Inc., Arizona, USA) and connected with a compressed nitrogen gas cylinder. The gas flow rate was adjusted to 8 L/min. The mouthpiece of the jet nebulizer was connected to an eight-stage Andersen Cascade Impactor (ACI) (Atlanta, GA, USA). The ACI was operated at the standard vacuum flow rate of 28.3 L/min (1 SCFM). The nebulizer was initially operated for 1 min, and the aerosol generated was directed to

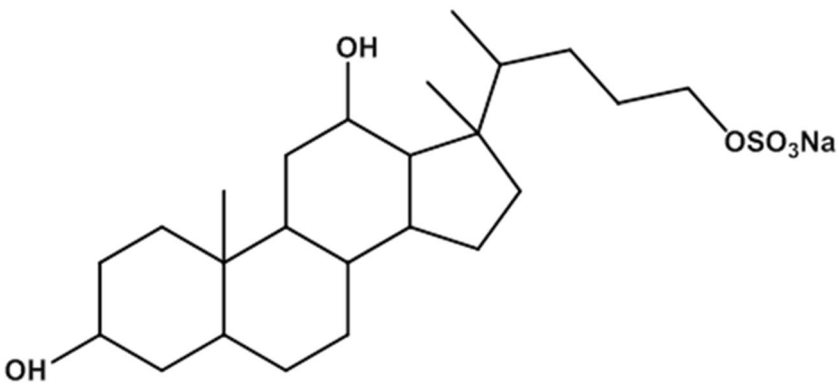

Fig. 1. Structure of sodium deoxycholate sulfate (SDCS)

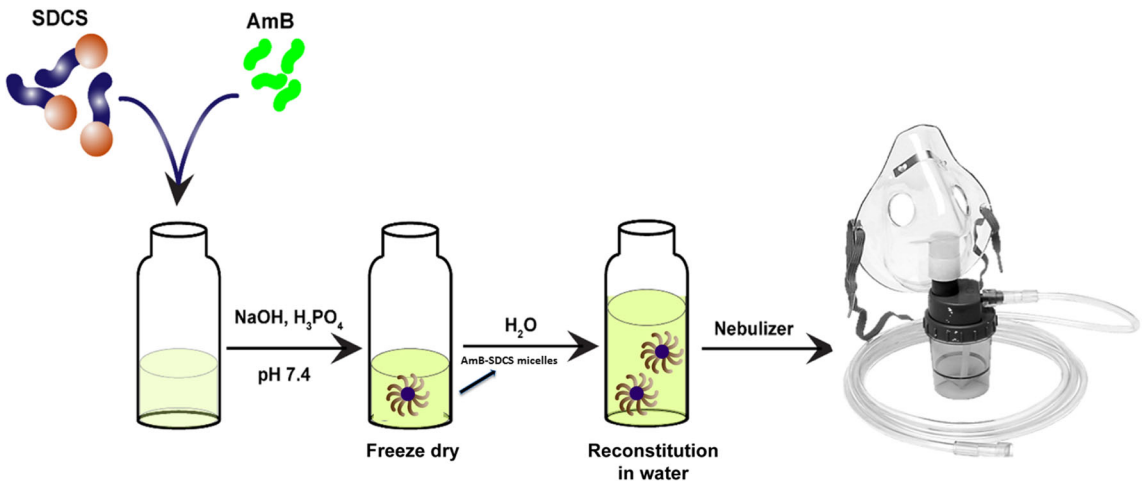

Fig. 2. Scheme for the preparation of inhalable nanomicelle formulation of AmB-SDCS

a fume hood as a standard protocol of USP29-NF24 which states that one delivery should be discharged to waste. After this nebulization period, the nebulizer was operated for a 2-min period to the ACI. The mass median aerodynamic diameter (MMAD) was calculated during the 1 to 3 min of nebulization time using linear interpolation of the cumulative mass distribution (17). The fine particle fraction (FPF) was calculated from the AmB that was deposited at each stage. FPF was defined as the particles fraction < 4.7 μm**.** All nebulization was carried out at room temperature to avoid any effect of temperature on particle deposition. Drug deposited at each stage and the metal inlet of the ACI was extracted by rinsing with 25 mL of a DMSO and methanol (1:9, *v*/*v*) solution. The amount of drug deposited at each stage as percent of loading dose was determined using high-performance liquid chromatography (HPLC). For the HPLC conditions, a mixture of acetate buffer (20 mM, pH 7.2) and acetonitrile, (60:40 *v*/*v*) for the mobile phase was used at a flow rate of 1 mL/min. The Micro Bondapak C18 column (Phenomenex, California, USA) (150 mm × 4.6 mm i.d., 5 μm) was used as the stationery phase. Detection was done with a UV detector at 405 nm. Similar chromatographic conditions were used to determine the % labeled amount of AmB in AmB-SDCS formulations for establishing uniformity of the lyophilized mixture prepared (18).

Potency of the AmB-SDCS Formulations

The microbiological method consisted of a cylinder plate agar diffusion assay using *Saccharomyces cerevisiae (S. cerevisiae*) as the test organism. *S. cerevisiae* with approximately 10^8 colony forming units (CFU)/mL was cultivated at 30°C on Sabouraud dextrose agar for 48 h. The yeast was suspended in 0.9% NaCl and diluted to obtain a turbidity of 25 ± 2% at 530 nm. A portion of this suspension (1 mL) was added to 100 mL sterile antibiotic medium 19 at 50°C and used as the pre-inoculated layer. Six stainless steel cylinders of uniform size (8 mm o.d. × 6 mm i.d. × 10 mm) were placed on the surface of the inoculated medium using a mechanical guide. The cylinders were filled with standard AmB and AmB-SDCS formulations. All plates were incubated at 30°C for 16–18 h. The inhibition zone diameters were measured using Antibiotic Zone Reader (Fisher-Lilly, Model 290, Virginia, USA), and the concentration of AmB was calculated from the standard curve. In case of not getting a perfect circle, measurement was repeated with new experiment and only perfect circles were included in the data presented. Zones were converted into concentration using standard curve of AmB that was drawn between concentration and inhibition zone using pure AmB following standard protocol of USP29-NF24 (19).

MIC and MFC

The minimum inhibitory concentration (MIC) and minimum fungicidal concentration MFC were determined using *S. cerevisiae*, *Cryptococcus neoformans (C. neoformans),* and *Candida albicans (C. albicans)* according to previously described work by McGinnis and Rinaldi (1996) (20). To ensure that the cultures for inoculation were in an active growth phase, fungi were sub-cultured on Sabouraud dextrose agar at 35°C for 24–48 h before the experiment. Stock microorganism suspensions were prepared in a sterile 0.9% NaCl solution and adjusted to give final concentrations in the range of 1×10^5 to 5×10^5 CFU/mL (90% transmittance at 530 nm). Standard AmB and AmB-SDCS reconstituted dry powder formulations were dissolved in 10% DMSO in sterile water at a concentration of 5000 μg/mL, respectively. The stock formulations were diluted subsequently with Antibiotic Medium 3 broth with concentrations between 0.004 and 10 μg/mL. Ten microliters of the inoculum and 100 μL of twofold serial dilutions of standard AmB and AmB-SDCS formulations at concentrations from 0.004 to 10 μg/mL were added to 96-well plates. The sterile medium was used as a negative control whereas the sterile medium with the inoculum was used as a positive control. The plates were incubated at 30°C for 48 h, and absorbance of the sample was measured at 570 nm using a microplate reader (Biohit BP 800, Helsinki, Finland).

Antileishmanial Assay

The *in vitro* antileishmanial activities of the AmB and AmB-SDCS formulations were evaluated against the promastigotes of *L. tropica* using the tetrozolium dye (MTT) assay as described by Mosmann (21) and later

modified by Niks and Otto (1990) (22). A stock solution of MTT (Sigma Chemical Co., St. Louis, Mo, USA) was prepared in a phosphate buffer saline (PBS) solution at 5 mg/mL and stored in the dark at 4°C. For the antileishmanial assay, 90 μL of the 2.5×10^6 cells/mL promastigotes was seeded in 96-well flat-bottom plates. Ten microliters of various concentrations of AmB, SDCS, and AmB-SDCS formulations was added to the wells, and the plates were incubated for 72 h at 23 ± 1°C. The well containing only 100 μL culture medium was taken as the blank. At the end of incubation, 10 μL of MTT was added to each well and the plates were again incubated for 3 h at 23 ± 1°C. Reaction was then stopped by the addition of 100 μL of 50% isopropanol and 10% sodium dodecyl sulfate in 0.1 N HCl. The plates were incubated for an additional 30 min under agitation at room temperature. The relative optical density (OD) was then measured at a wavelength of 570 nm using a 96-well microplate reader (Bio-Tek ELx 800™, Instruments, Inc. Winooski, VT, USA). The absorbance of the formazan produced by the action of mitochondrial dehydrogenases of metabolically active cells was correlated with the number of viable cells (21,22). All experiments were performed in triplicate. The results are reported as the IC_{50} ± SEM of each of the three independent experiments. Half maximum inhibitory concentration (IC_{50}) values of potential inhibitors (≥ 50%) were obtained with the help of the non-linear regression analysis program of GraphPad Prism 5.0 Software Inc., San Diego, CA, USA.

Cytotoxicity Assay Using Respiratory and Kidney Cells

The MTT colorimetric assay as described by Mosmann (1983) (21) and modified by Edmondson et al., (1988) (23) was used to examine the cytotoxicity of the AmB-SDCS formulations as well as AmB and SDCS on human bronchial epithelial cells (Calu-3), lung adenocarcinoma cell line (A549), alveolar macrophage (AM) NR8383 cell line, and human embryonic kidney cell lines (293T/17). Live mitochondria transformation from MTT to formazan was measured using spectrofluorimetry. Calu-3, A549, AM NR8383, and kidney (293T/17) cells were distributed in 96-well plates at a density of 1×10^5 cells/well in 100 μL of completed medium and allowed to attach overnight at 37°C and 5% CO_2 with 95% relative humidity. After 24 h, the medium (100 μL) was replaced with medium containing various concentrations of the different formulations of AmB-SDCS (1 to 16 μg/mL) or an equivalent concentration of AmB. After incubation for 24 h, 50 μL (1.25 mg/mL) of MTT was added and further incubated for 4 h at 37°C in 5% CO_2 and 95% humidity. The solutions were removed from the 96-well plates and 100 μL of DMSO was added to dissolve formazan crystals. The ODs were measured at 570 nm using a microplate reader. The percentage of surviving cells was calculated from the following formula:

$$\%\text{surviving cells} = (OD_{treated}/OD_{control}) \times 100$$

The number of viable cells in the treated wells were compared to those in the untreated wells and estimated as percent viability.

Cellular Uptake by Alveolar Macrophages

The NR8383 cell line is established from normal alveolar macrophage cells obtained by lung lavage. NR8383 cells were cultured and sub-cultured from single cells by limiting dilution, and then sub-cultured from soft agar three times. The cells exhibit characteristics of macrophage cells. Alveolar macrophages were cultured in F12K supplemented with 15% heat-inactive fetal bovine serum, 50 units/mL penicillin, and 50 μg/mL streptomycin. They were incubated in a 5% CO_2 and 95% humidity incubator at 37°C. AmB-SDCS formulation was reconstituted in water to obtain a concentration of 1 mg/mL of AmB. Particle imaging was carried out using quantum dot nanoparticles. Lumidot® 640 (10 μg/mL) was added to stain the reconstituted AmB-SDCS formulation (4 μg/mL). The concentration of Lumidot 640® (Lumidot 640®, Sigma-Aldrich, St. Louis, USA) was used on the basis of the MTT assay performed to determine the safe concentrations. The mixture was vortexed for 5 min to ensure complete mixing. The AmB-SDCS formulation with Lumidot™ 640, AmB-SDCS formulation with Lumidot™ 640, and NR8383 cells were incubated in 12-well plates for 8 h. The cells were separated by centrifugation, washed four times with sterile PBS, and examined *via* confocal laser scanning microscopy (Olympus Fluoview FV 3000, Olympus Corporation, Tokyo, Japan).

Molecular Modeling Simulations

In order to predict the plausible interactions and the dynamics of the AmB-SDCS formulation, a short production run was carried out. The compounds were drawn using the builder module in Molecular Operating Environment (MOE) 2013.08 software (Chemical Computing Group ULC, 1010 Sherbooke St. West, Suite #910, Montreal, QC, Canada, H3A 2R7, 2017) and charged and minimized using the Merck Molecular Force Field that is used to define various characteristics of the small molecules, including bond angles, bond lengths, and dihedral angles (MMFF94s) implemented in the MOE. The binding mode of AmB and SDCS was established using the docking protocol mentioned earlier (24).

In order to understand the dynamics, two different dynamic simulations were performed: one with AmB and the other with AmB-SDCS complex. The electrostatic charges were assigned using the generalized AMBER force field (GAFF) implemented in AMBER16 (latest version of molecular dynamics simulation software) (25). An arbitrary water box of 10 Å was built around the complex and was solvated using the single point calculation water model. Next, the formats required in AMBER software suite to perform molecular dynamics simulation, prmtop and incprd, were generated. These formats represent structural and spatial details of the molecules, respectively. The system was minimized to relax the system and remove the potential clashes. Afterwards, the entire system was subjected to gradual heating from 0 to 300 K to achieve a stable temperature followed by equilibration of 50 ps. A production run of 10 ns was carried out at a constant temperature of 300 K and 1 atm. For the analysis of trajectories, a package implemented in AMBERTOOLS (CPPTRAJ) was used (Roe and Cheatham III, 2013) (26). The entire visual analysis was

performed using visual molecular dynamics (VMD) and Chimera, molecular visualization software that are used to render trajectories obtained from simulation (27,28).

RESULTS

Aerosol Parameters of AmB-SDCS Reconstituted Formulations

In vitro deposition of reconstituted AmB-SDCS lipid formulations was carried out using the ACI by jet nebulization. The ACI can separate particles by their aerodynamic size at each stage collecting particle sizes larger than the effective cut-off diameter, whereas smaller sizes pass through to the lower stage. Table I shows various aerosol parameters for the AmB-SDCS formulations. The MMAD of AmB-SDCS formulations was in the range of 0.9–1.6 μm whereas GSD was in the range of 1.4–2.1. FPF was the amount of AmB less than 4.7 μm and its value was in the range of 70.3–86.5**%.** The % labeled amount of AmB for all formulations as determined by HPLC was in the range of 98.7–101.4% which indicated uniformity in all of the formulations. The drug deposited on various stages was determined by HPLC as shown in Table II. Approximate dose left in the nebulizer was about 40% with no evidence of any precipitation or degradation. It is therefore an evidence of AmB stability during the nebulization period.

Potency of the AmB-SDCS Formulations

A comparison of the AmB-SDCS reconstituted formulations with the same concentration of standard AmB against *S. cerevisiae* is shown in Fig. 3a. The potency of the AmB-SDCS formulations was in the range of 95.6–106.1**%.** SDCS alone did not inhibit the growth of fungus. It is evident that the values were almost equivalent with the standard AmB with negligible difference indicating no effect of the lipid carrier on the potency of AmB.

MIC and MFC

Table III shows the MIC and MFC values of AmB, SDCS, and AmB-SDCS formulations against *S. cerevisiae*, *C. neoformans*, and *C. albicans*. A significant decrease in MIC and MFC was observed in the AmB-SDCS formulations (1:2 and 1:3 M ratios) from that of AmB. The MIC was reduced about 8-fold, whereas the MFC was reduced by 4- to 24-fold. No fungal susceptibility was found for the lipid carrier (SDCS) alone. Previously reported values of MIC of AmB against *S. cerevisiae* were 0.5–1 μg/mL (29) and 0.125–4 μg/mL (30), whereas in the case of AmB-deoxycholate and liposomal AmB, these values were 0.31–0.63 and 0.63–2.5 μg/mL, respectively (31). The MFCs for AmB, liposomal AmB, and cholesterol containing liposomal AmB were 0.4–1.6, 0.8, and 1.6–3 μg/mL, respectively.

The MIC and MFC determined by Chuealee et al., (2011) (18) with AmB incorporated in liquid crystals against *C. neoformans* using various lipid derivatives were found to be 0.08–0.15 and 0.08–0.6 μg/mL, respectively. Against *C. albicans*, the reported MIC and MFC values were 0.08–0.15 and 0.08–0.6 μg/mL, respectively, whereas in the case of *S. cerevisiae*, the results obtained were 0.08–1.5 and 0.08–1.6 μg/mL, respectively. The results of the MIC and MFC using the AmB-SDCS formulations were in the ranges stated above.

Antileishmanial Activity

The antileishmanial activities of the AmB-SDCS formulations and AmB are shown in Fig. 3b. The pharmacological target of AmB in Leishmania is ergosterol in the fungal cell membrane. The activities improved with AmB-SDCS; the IC_{50} was 0.021 μM for the 1:2 formulation and 0.035 μM for the 1:3 formulation. These results were significantly lower than AmB (0.135 μM). In the case of other formulations, IC_{50} was also lower compared to AmB.

Cytotoxicity Assay against Respiratory and Kidney Cell Lines

AmB-SDC (1:2 M ratio) and AmB-SDCS lipid formulations were employed to determine their toxicity on lung cell lines including Calu-3, A549, and NR8383 as well as kidney cells (T-293/17) using concentrations ranging from 1 to 16 μg/mL by MTT reduction assay following 24-h exposure. Figure 4 shows the percent viability against the cells at various concentrations. The effective AmB concentration in the blood stream is 1 μg/mL with a similar concentration in the lungs. Typical *in vitro* concentrations of AmB for drug delivery strategies should be 8–16 times the *in vivo* therapeutic concentrations, and similar concentrations were used in the study (32). The pure SDCS lipid carrier was found to be non-toxic for all concentrations used with cell viability nearly 100% in all cases.

The cell viability of the Calu-3 cells was nearly 100% for concentrations of 1–4 μg/mL and all AmB-SDCS formulations demonstrated very low toxicity at concentrations of 8 μg/mL with cell viability falling in the range of 80–90% in all cases (Fig. 4a). A slight decrease in viability was observed

Table I. Aerosol Parameters of AmB-SDCS Formulations Reconstituted in Distilled Water 5 mg/ml (Mean ± S.D., $n = 5$)

Molar ratio of AmB-SDCS formulation	MMAD (μm)	% FPF (< 4.7 μm)	GSD	% Labeled amount of AmB
1:1	0.9 ± 0.2	86.5 ± 1.4	1.7 ± 0.1	99.2 ± 1.4
1:2	1.0 ± 0.2	81.4 ± 2.6	2.1 ± 0.2	98.7 ± 0.8
1:3	1.2 ± 0.1	75.6 ± 3.4	1.7 ± 0.2	100.5 ± 1.1
1:4	1.4 ± 0.1	72.1 ± 3.7	1.5 ± 0.1	101.4 ± 2.2
1:5	1.6 ± 0.2	70.3 ± 2.9	1.4 ± 0.2	98.9 ± 0.6

GSD geometric standard deviation, *AmB* amphotericin B, *SDCS* sodium deoxycholate sulfate

Table II. Deposition Profile of AmB as Percent of Loading Dose on Each Stage of ACI for AmB-SDCS Formulations (Mean ± S.D., $n = 5$)

Stage of ACI	Cut-off size (μm)	Deposition as % of dose loaded for AmB-SDCS formulations				
		1:1	1:2	1:3	1:4	1:5
S_0	9	2.3 ± 0.6	3.3 ± 1.1	1.9 ± 0.5	4.4 ± 0.6	3.9 ± 0.8
S_1	5.8	4.3 ± 1.0	5.6 ± 1.5	8.3 ± 0.6	9.3 ± 1.3	9.6 ± 0.4
S_2	4.7	1.3 ± 1.1	1.2 ± 0.6	1.9 ± 0.8	1.9 ± 0.7	1.6 ± 0.6
S_3	3.3	2.1 ± 0.8	1.8 ± 0.6	2.5 ± 0.4	3.1 ± 0.4	3.3 ± 0.8
S_4	2.1	2.3 ± 1.7	2.9 ± 0.5	3.2 ± 1.1	2.9 ± 0.8	3.1 ± 1.2
S_5	1.1	5.0 ± 1.1	4.1 ± 0.9	6.2 ± 0.9	6.3 ± 0.9	5.5 ± 0.9
S_6	0.7	15.2 ± 0.9	14.4 ± 1.5	9.7 ± 1.6	11.2 ± 1.2	11.9 ± 1.5
S_7	0.4	15.6 ± 1.0	15.3 ± 1.3	13.5 ± 0.9	10.6 ± 1.4	8.3 ± 1.6
Total drug recovery in the ACI		48.1 ± 1.1	48.6 ± 1.0	47.2 ± 0.9	49.7 ± 0.9	47.2 ± 1.0

ACI Andersen Cascade Impactor, *AmB* amphotericin B, *SDCS* sodium deoxycholate sulfate

at 16 μg/mL, especially for the 1:3, 1:4, and 1:5 AmB-SDCS formulations where the viability dropped to less than 80%. In the case of AmB-SDC, cell viability was below 70%. This indicated that all AmB-SDCS formulations were relatively non-toxic to the lung cell line Calu-3 but better than the market formulation of Fungizone®. In the case of A549 cell lines, no toxicity was observed at 1–4 μg/mL with cell viability at 100% except with formulation 1:5 where a slight reduction in toxicity was observed. A similar pattern was observed for the 1:5 formulation with reduced viability at 8 μg/mL, whereas for all other formulations, it was nearly 90% showing negligible toxicity. All of the formulations were much better than the AmB-SDC which the cell viability was reduced to less than 75% at 8 and 16 μg/mL. The AmB-SDCS (1:2) did not show toxicity even at higher concentrations (*i.e.*, 16 μg/mL**)** and the cell viability was 91.4% (Fig. 4b). The viabilities of the NR8383 cells at 24-h incubation with AmB-SDCS formulations were 100% for 1–2 μg/mL and ~ 90% at 4 μg/mL, whereas the viability was slightly reduced to 80% at 8 μg/mL for the 1:2 and 1:3 formulations (Fig. 4c). In the case of the 1:1, 1:4, and 1:5 AmB-SDCS formulations, the cell viabilities were lower than 80%. Cell viability sharply reduced to below 65% at 8 μg/mL and, while less than 80% at 4 μg/mL for AmB-SDCS, it dropped to less than 50% at 16 μg/mL. Nephrotoxicity was assessed *in vitro* using human kidney cells (T293/17). No cell damage was observed at 1 and 2 μg/mL, whereas slight toxicity was observed at 4 μg/mL (Fig. 4d). At higher concentration (*i.e.*, 8 μg/mL), cell viability was 80–90% which showed protection provided by the lipid carrier to kidney cells. At 16 μg/mL, viability was still above 80% for the 1:2 and 1:3 formulations, whereas it was below 80% in the 1:3 and 1:4 formulations. In the case of formulation 1:5, cell damage was increased with viability to less than 70%. For AmB-SDC, cell viability dropped below 70% at 8 and 16 μg/mL.

Cellular Uptake of AmB-SDCS Reconstituted Formulation by AM NR8383 Cells

AmB-SDCS formulation (1:2) was reconstituted in distilled water followed by staining with Lumidot® 640. The AmB-SDCS lipid formulation images were taken in fluorescence mode. The particle size of the AmB-SDCS (1:2) was about 200 ± 2.5 nm. The data harmonized with the size

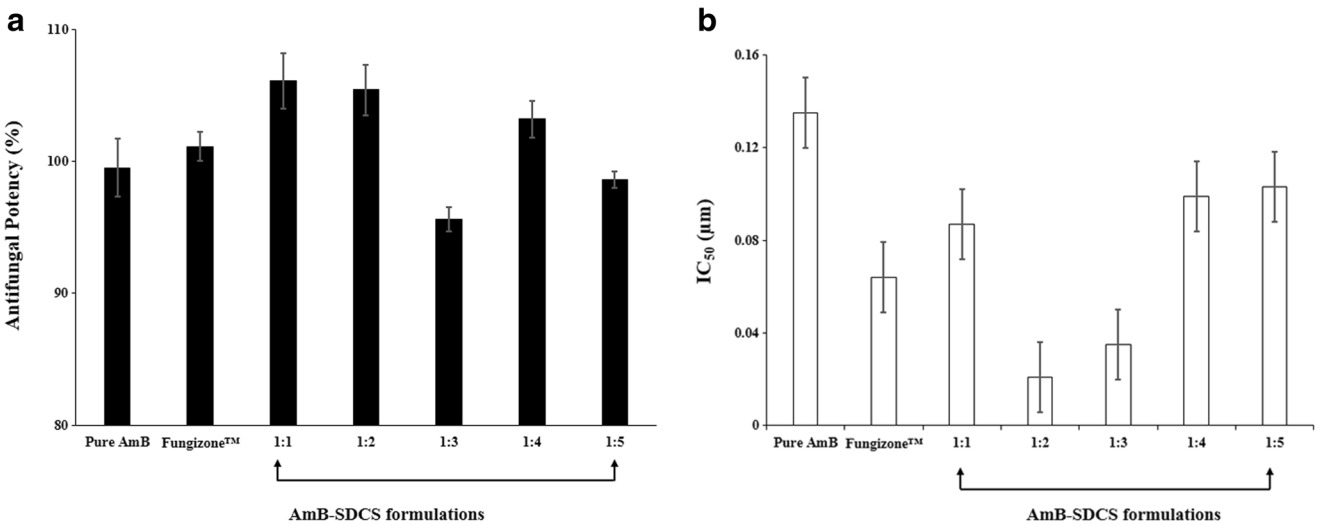

Fig. 3. Antifungal potency (**a**) antileishmanial activity in context of $IC_{50} \pm SEM$ (**b**) of AmB, Fungizone™, and AmB-SDCS formulations in different molar ratios

Table III. MIC and MFC Values of AmB, SDCS, and AmB-SDCS Lipid Formulations

Molar ratio of AmB-SDCS formulation	*S. cerevisiae*		*C. neoformans*		*C. albicans*	
	MIC (μg/mL)	MFC (μg/mL)	MIC (μg/mL)	MFC (μg/mL)	MIC (μg/mL)	MFC (μg/mL)
AmB	0.02	0.04	0.08	0.16	0.08	0.24
SDCS	–	–	–	–	–	–
1:1	0.02	0.02	0.02	0.02	0.08	0.08
1:2	0.005	0.005	0.01	0.01	0.01	0.01
1:3	0.01	0.01	0.02	0.02	0.01	0.01
1:4	0.01	0.02	0.04	0.08	0.02	0.06
1:5	0.01	0.02	0.04	0.08	0.04	0.12

MIC minimum inhibition concentration, *MFC* minimum fungicidal concentration, *AmB* amphotericin B, *SDCS* sodium deoxycholate sulfate

measurement obtained after reconstitution. The AmB-SDCS particles were observed as round shaped with a narrow size distribution owing to the low polydispersity index (PDI), *i.e.*, 0.23 ± 0.02, giving uniform particles in the liquid dispersion (22). The zeta potential of the aforesaid AmB-SDCS formulation was -39.2 ± 2.6 mV whereas for Fungizone, it was 21.0 ± 2.3 mV. PDI value for Fungizone was 0.39 ± 0.05 whereas particle size was 201.3 ± 7.4 nm. Phagocytosis was observed following incubation of the NR8383 cells for 8 h, and the intensity of fluorescence revealed phagocytosis of AmB-SDCS inside the cells. Figure 5 indicates the NR8383 cells could efficiently phagocytose the particles stained with Lumidot® 640. No evidence of damage to the cells was observed, and all cells were shown to retain their normal morphology showing no toxic effects of the lipid carrier SDCS.

MD Simulation

In order to understand the real-time dynamics of the AmB-SDCS complex, MD simulations of the AmB in water and in the AmB-SDCS complex were carried out. In a previous study, we reported the docking simulation of the AmB-SDCS complexes and the results were found to be in decent agreement with the nuclear magnetic resonance results (24). In the present study, we performed MD simulations of the AmB-SDCS complex to understand the real-time dynamics and the plausible mechanism of the facilitation of the AmB activity mediated by the SDCS molecule. The visual analysis of the complex suggests that the SDCS molecules wrap around the AmB molecules making both polar and apolar contacts. Figure 6 depicts the binding mode of AmB-SDCS in the presence of water. The sulfate moiety SDCS molecule 1 (SDCS_1) depicts two hydrogen bonds with the hydroxyl groups present within the polyol part of the AmB.

DISCUSSION

Aerosol powders with MMAD ranging from 1 to 5 μm are considered the optimal size for deposition into the deep airways as far as the alveoli which is the point of focus in targeting diseased lung (33). Geometric standard deviation (GSD) represents the spread of the particles in the formulation (34). The GSD values obtained from all of the AmB-SDCS formulations were above 1.25 which indicated a

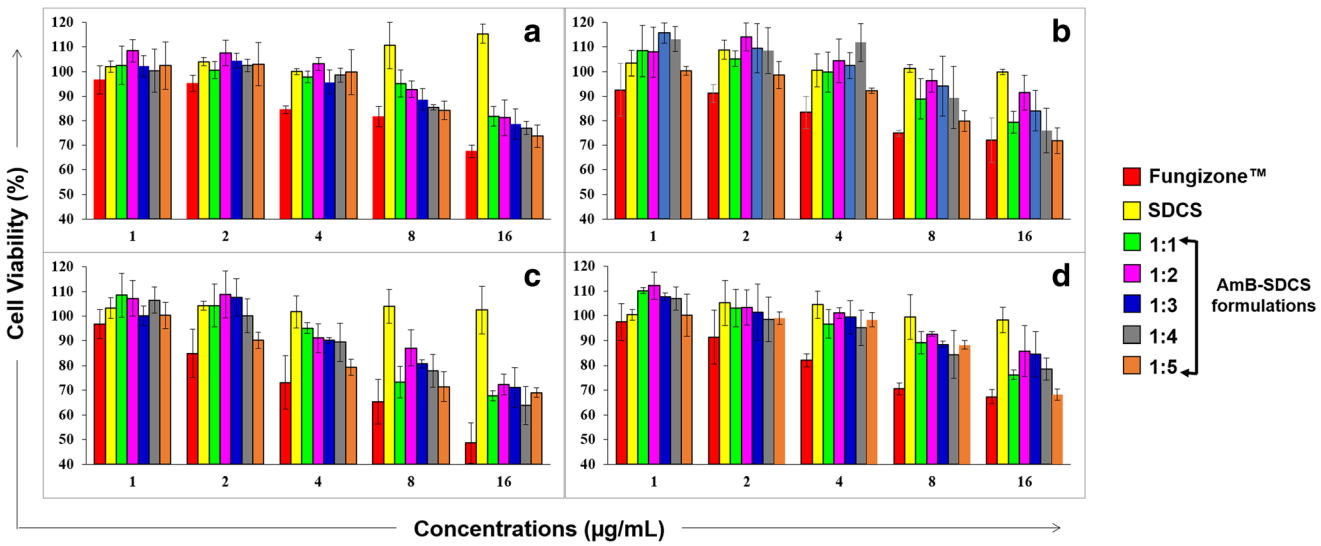

Fig. 4. Viability of (**a**) Calu-3, (**b**) A549, (**c**) AM NR8383, and (**d**) T 293/17 cell lines followed by 24-h incubation with AmB-SDC and AmB-SDCS formulations in various molar ratios (mean ± S.D., $n = 4$)

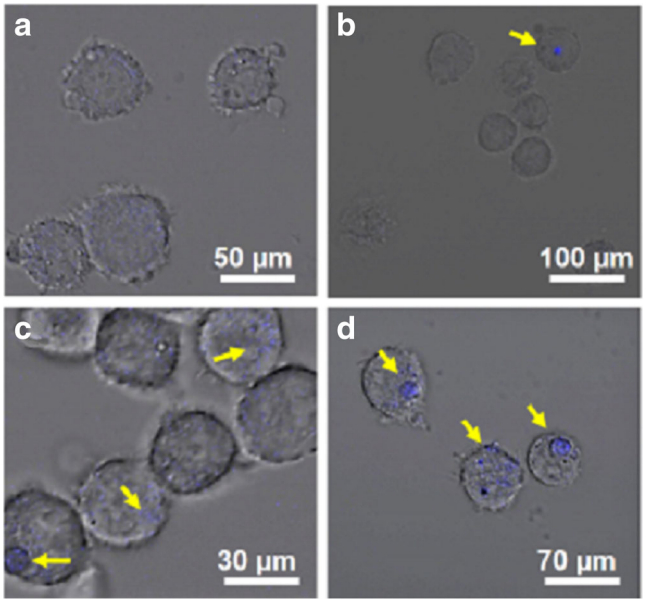

Fig. 5. Phagocytosis of AM NR8383 cells incubated with AmB-SDCS in reconstituted formulation stained with Lumidot® 640 for 8 h; **a** Macrophage cells. **b** Fungizone-treated cells with Lumidot®. **c** Lumidot® 640-treated cells. **d** Cells treated Lumidot®-tagged AmB-SDCS formulation. Lumidot® is pointed with yellow arrows

polydisperse formulation (35). The AmB stability and concentration assay of AmB in the formulation is dependent upon the dosage form and drug release parameters with respect to time (36). The drug concentration assays of all formulations were indicative of uniformity as well as stability of the formulations without any degradation of AmB during nebulization. Aerodynamic diameters less than 4.7 µm suggested that the formulations were suitable to deliver the drug into the lower airways as far as the alveoli because they were deposited in stages 4–7 of the ACI. The residual solution was also evaluated for activity as well as physicochemical

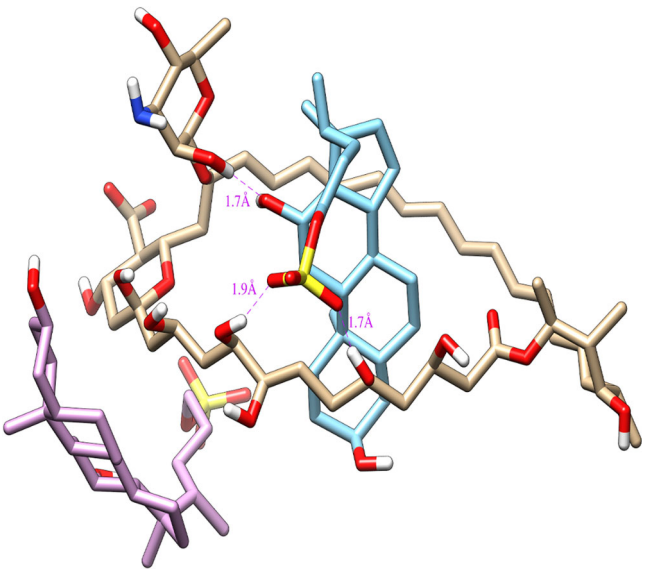

Fig. 6. The simulated pose of the AmB-SDCS complex (1:2 M ratio) in the water. The AmB is presented as golden sticks while SDCS_1 and SDCS_2 are depicted in cyan and purple sticks respectively

parameters, and all the aspects were maintained in the residue left in the nebulizer with no evidence of any precipitation. A slight decrease was observed in the FPF with increasing molar ratio of SDCS. MMAD showed an increasing trend with increased molar ratio of lipid carrier SDCS. GSD of all AmB-SDCS formulations was 1.4–2.1 which showed polydisperse distribution. A relatively low MMAD (1–2 µm) with high FPF (70–85%) is considered as an efficient aerosolized delivery for AmB-SDCS formulations. The total drug recovery in the ACI was 47.2 to 49.7% (Table II). On the other hand, no AmB degradation was observed in the nebulizer. Low AmB recovery can be attributed to the drug loss in the tubing, mouthpiece adapter, and inlet of the ACI during nebulization. It was quite evident that SDCS also has no contribution in enhancing the AmB potency either by transporting AmB inside the fungal cells or facilitating more penetration into the fungal membranes (18). SDCS played a pivotal role only in dissolving the poorly soluble hydrophobic AmB into water. The results of MIC and MFC indicated improvement of AmB activity by the lipid career SDCS and its sole role in the solubility of hydrophobic AmB. MFC values mentioned in the literature may vary depending on the source of AmB and fungal isolates as aforementioned in the results**.** The MIC and MFC results suggest that the lipid career was essential for the solubility of AmB which resulted in an association of the lipid career with the fungal cell membrane by either facilitating the transfer of AmB along with lipid career or inducing the formation of ionophores (37).

The clinical applications of AmB are limited due to its high nephrotoxicity (38). The incidence of nephrotoxicity reported with conventional AmB-SDC is 49–65% (39). To minimize this toxicity, lipid formulations of AmB were prepared using various molar ratios of the lipid carrier SDCS which was synthesized in house with a natural precursor. The results indicated that AmB-SDCS formulations were non-toxic in comparison to AmB-SDC. A comparatively weak barrier was provided by the micelle system to the lipid bilayers in comparison to liposomes or lipid nanoparticles (LPNs). The AmB release form micelles may be faster compared to Ambisome® or LPNs (40). However, a strong interaction between AmB and lipids, like phospholipids and cholesterol, can slow the AmB release from LPNs or Ambisome® (41). Consequently, liposomes and LPNs can decrease the cytotoxicity of the drugs entrapped in them (42). In this case, it is quite possible that lipid formulations form a more stable micellar system than AmB-SDC (24) which results in a slower release of AmB, with an ultimately lower toxicity to the kidney cells. AmB-SDCS formulations were less toxic to all lung cell lines, indicating formation of a more stable micelle system. Therefore, release of AmB from the AmB-SDCS formulations was slower, resulting in lower toxicity for all cell lines up to 8 µg/mL.

This trend in antileishmanial and antifungal activity can be explained on the basis of size *versus* encapsulation efficiency of the formulations (24,43). At lower drug to encapsulant ratios (*e.g.*, 1:4 and 1:5), less drug is entrapped inside the micelle systems and the particle size is increased due to aggregated layers of encapsulant on the surface of the micelles that leads to reduced activity. At lower encapsulant to drug ratios (*e.g.*, 1:1), the lower amount of drug is taken up

in the micelle system and it also leads to reduced activity (43). Therefore, an optimal drug to encapsulant ratio (*e.g.*, 1:2 and 1:3) can provide a size *versus* drug loading which can interact with the membrane of the microbe and deliver a high payload of the drug (44,45). Lower drug activity against Leishmania parasites is ascribed to the coat of phospholipoglycans on the membranes along with the slow efflux phenomenon which is evident in resistant strains (46). The activity of AmB-SDCS formulations may be attributed to their ability to interact with the outer coat of the parasite and deliver the drug. It was recently reported that poly (lactide-co-glycolic acid) nanoparticles were far better than the conventional AmB formulation (*i.e.*, Fungizone®). Similarly, markedly increased leishmanial activity was observed by Javed et al., (2015) (40) using lecithin-based nanocarriers of AmB. The activity in this case was significantly increased for liposomal formulations of lecithin-coated nanoparticles of AmB.

It was reported by Kanchan and Panda (47) that nanoparticles in the size range of 200–600 nm could be efficiently phagocytosed by macrophage cells, and the same was observed for an AmB-SDCS formulation where the size was also in the same range with efficient phagocytosis. They also observed that maximum uptake was observed between 6 and 24 h, and similar results were obtained for AmB-SDCS where phagocytosis was observed following an 8-h incubation. It is also pertinent to mention that the size and surface chemistry of nanoparticles have important influence on the uptake of particles, and hydrophobic particles have a tendency to adhere to the cell surface (48,49). The results support the view that the AmB-SDCS lipid formulation could be efficiently phagocytosed by alveolar macrophage cells *in vitro*, and the lipid formulation of AmB can be highly effective in treating pulmonary fungal infection by targeting macrophages as this is the main store house for fungal cells in the lungs.

In the docking simulations, intramolecular hydrogen bonding might result in the formation of a molecular environment which might enhance the overall polarity of the molecule. These hydrogen-bonding interactions partially explain the delayed release of the drug which resulted in the reduced toxicity of our proposed formulation. Moreover, the hydroxyl group of the SDCS_1 also complements the anchorage provided by the sulfate moiety. The hydroxyl group of the ligand is involved in hydrogen-bonding interaction with the hydroxyl group at the mycosamine moiety of the AmB molecule. The other SDCS molecular SDCS_2 presents a number of hydrogen-bonding interactions with different groups of the AmB molecule. However, these interactions were dynamic in nature and their occupancy was very low. In the most populous sample of the trajectory (Fig. 6), the hydroxyl group of the SDCS_2 is present within 5 Å of the hydroxl group of the AmB molecule, which suggests the probability of formation of hydrogen bonding. We assume that this particular complexation might facilitate the transmission of the AmB molecule through the fungal cell wall which partially explains the enhanced fungicidal activity of the AmB-SDCS complex. Another interesting observation is the increased surface area of the complex during the simulation, which is evident by the increase in the radius of gyration, which may contribute towards the increased absorption of the drug by the Leishmania parasite.

CONCLUSIONS

AmB-SDCS formulations in various molar ratios were found to be suitable for nebulization for drug delivery into the lungs. AmB-SDCS had an equivalent potency compared to AmB. The MIC and MFC was significantly reduced against *S. cerevisiae*, *C. neoformans*, and *C. albicans*. AmB-SDCS was also successfully phagocytosed by AM NR8383 cells. The tests for bioactivity and *in vitro* cytotoxicity demonstrated that SDCS was a safe lipid carrier for pulmonary delivery of AmB with no evidence of toxicity for respiratory and kidney cell lines. Antileishmanial activity was also improved by all AmB-SDCS formulations at 1:2 and 1:3 ratios. Molecular modeling further complemented the results of bioactivity suggesting the formation of probable hydrogen bonding in the AmB-SDCS complex which facilitates the transmission of the AmB molecule through the fungal cell wall. It is concluded that AmB-SDCS-based nanomicellar system is better than the conventional liposomal formulations in the context of solubility, safety, bioactivity, and cost and can find future implications in designing therapeutically safe and effective formulations for lung delivery of AmB.

ACKNOWLEDGEMENTS

The authors also acknowledge the Computational Chemistry Unit, Dr. Panjwani Centre for Molecular Medicine and Drug Research, International Centre for Chemical and Biological Sciences, University of Karachi, Karachi-75270, Pakistan, for the docking studies.

Funding information This research was funded by a grant from the 2014 scholarship awards for Masters and Ph.D. studies under Thailand's Education Hub for Southern Region of ASEAN countries (TEH-AC).

COMPLIANCE WITH ETHICAL STANDARDS

Conflict of Interest The authors declare that they have no conflict to declare.

REFERENCES

1. Kontoyiannis DP, Marr KA, Park BJ, Alexander BD, Anaissie EJ, Walsh TJ, et al. Prospective surveillance for invasive fungal infections in hematopoietic stem cell transplant recipients, 2001–2006: overview of the transplant-associated infection surveillance network (TRANSNET) database. Clin Infec Dis. 2010;50:1091–100.
2. Park BJ, Pappas PG, Wannemuehler KA, Alexander BD, Anaissie EJ, Andes DR, et al. Invasive non-Aspergillus mold infections in transplant recipients, United States, 2001–2006. Emerg Infect Dis. 2011;17:1855–64.
3. Dupont B. Overview of the lipid formulations of amphotericin B. J Antimicrob Chemoth. 2002;49:31–6.
4. Hamill RJ. Amphotericin B formulations: a comparative review of efficacy and toxicity. Drugs. 2013;73:919–34.
5. Gallis HA, Drew RH, Pickard WW. Amphotericin B: 30 years of clinical experience. Rev Infect Dis. 1990;12:308–29.
6. Ellis D. Amphotericin B: spectrum and resistance. J Antimicrob Chemoth. 2002;49:7–10.

7. Laniado-Laborín R, Cabrales-Vargas MN. Amphotericin B: side effects and toxicity. Rev Iberoam Micol. 2009;26:223–7.
8. Walsh TJ, Finberg RW, Arndt C, Hiemenz J, Schwartz C, Bodensteiner D, et al. Liposomal amphotericin B for empirical therapy in patients with persistent fever and neutropenia. New Engl J Med. 1999;340:764–71.
9. Javed I, Hussain SZ, Shahzad A, Khan JM, Rehman M, Usman F, et al. Lecithin-gold hybrid nanocarriers as efficient and pH selective vehicles for oral delivery of diacerein—in-vitro and in-vivo study. Colloids Surf B Biointerfaces. 2016;141:1–9.
10. Cagnoni PJ, Walsh TJ, Prendergast MM, Bodensteiner D, Hiemenz S, Greenberg RN, et al. Pharmacoeconomic analysis of liposomal amphotericin B versus conventional amphotericin B in the empirical treatment of persistently febrile neutropenic patients. J Clic Oncol. 2000;18:2476–83.
11. Scholar EM, Pratt WB. The antimicrobial drugs. Oxford: Oxford University Press; 2000.
12. Bennett JE, Dolin R, Blaser MJ. Principles and practice of infectious diseases. Amsterdam: Elsevier Health Sciences; 2014.
13. Torrado J, Espada R, Ballesteros M, Torrado-Santiago S. Amphotericin B formulations and drug targeting. J Pharm Sci. 2008;97:2405–25.
14. Baginski M, Czub J. Amphotericin B and its new derivatives-mode of action. Curr Drug Metab. 2009;10:459–69.
15. Kakinen A, Javed I, Faridi A, Davis TP, Ke PC. Serum albumin impedes the amyloid aggregation and hemolysis of human islet amyloid polypeptide and alpha synuclein. Biochim Biophys Acta. 2018; https://doi.org/10.1016/j.bbamem.2018.01.015.
16. Gangadhar KN, Adhikari K, Srichana T. Synthesis and evaluation of sodium deoxycholate sulfate as a lipid drug carrier to enhance the solubility, stability and safety of an amphotericin B inhalation formulation. Int J Pharm. 2014;471:430–8.
17. Sham JO-H, Zhang Y, Finlay WH, Roa WH, Löbenberg R. Formulation and characterization of spray-dried powders containing nanoparticles for aerosol delivery to the lung. Int J Pharm. 2004;269:457–67.
18. Chuealee R, Aramwit P, Noipha K, Srichana T. Bioactivity and toxicity studies of amphotericin B incorporated in liquid crystals. Eur J Pharm Sci. 2011;43:308–17.
19. US Pharmacopeial Convention, USP29-NF24. Guidline no 66: antibiotics, micorbial assays. Rockville: USP; 2006.
20. McGinnis MR, Rinaldi MG. Antifungal drugs: mechanisms of action, drug resistance, susceptibility testing, and assays of activity in biological fluids. Antibiotics in laboratory medicine. Baltimore: The Williams & Wilkins Co; 1996. p. 176–211.
21. Mosmann T. Rapid colorimetric assay for cellular growth and survival: application to proliferation and cytotoxicity assays. J Immunol Methods. 1983;65:55–63.
22. Nikš M, Otto M. Towards an optimized MTT assay. J Immunol Methods. 1990;130:149–51.
23. Edmondson JM, Armstrong LS, Martinez AO. A rapid and simple MTT-based spectrophotometric assay for determining drug sensitivity in monolayer cultures. Methods Cell Sci. 1988;11:15–7.
24. Usman F, Ul-Haq Z, Khalil R, Tinpun K, Srichana T. Pharmacologically safe nanomicelles of amphotericin B with lipids: nuclear magnetic resonance and molecular docking approach. J Pharm Sci. 2017;106:3574–82.
25. Case DA, Betz RM, Cerutti DS, Cheatham TE III, Darden TA, Duke RE, et al. AMBER. San Francisco: University of California; 2016.
26. Roe DR, Cheatham TE III. PTRAJ and CPPTRAJ: software for processing and analysis of molecular dynamics trajectory data. J Chem Theory Comput. 2013;9:3084–95.
27. Chimera U, Pettersen EF, Goddard TD, Huang CC, Couch GS, Greenblatt DM, et al. A visualization system for exploratory research and analysis. J Comput Chem. 2004;25:1605–12.
28. Humphrey W, Dalke A, Schulten K. VMD: visual molecular dynamics. J Mol Graph. 1996;14:33–8.
29. Echeverría-Irigoyen MJ, Eraso E, Cano J, Gomáriz M, Guarro J, Quindós G. Saccharomyces cerevisiae vaginitis: microbiology and in vitro antifungal susceptibility. Mycopathologia. 2011;172:201–5.
30. Barchiesi F, Arzeni D, Compagnucci P, Di Francesco LF, Giacometti A, Scalise G. In vitro activity of five antifungal agents against clinical isolates of Saccharomyces cerevisiae. Med Mycol. 1998;36:437–40.
31. Ralph E, Khazindar A, Barber K, Grant C. Comparative in vitro effects of liposomal amphotericin B, amphotericin B-deoxycholate, and free amphotericin B against fungal strains determined by using MIC and minimal lethal concentration susceptibility studies and time-kill curves. Antimicrob Agents Ch. 1991;35:188–91.
32. Yu B, Okano T, Kataoka K, Kwon G. Polymeric micelles for drug delivery: solubilization and haemolytic activity of amphotericin B. J Control Release. 1998;53:131–6.
33. Rau JL. Respiratory care pharmacology. Maryland Heights: Mosby Incorporated; 2002.
34. Mitchell JP, Nagel MW, Wiersema KJ, Doyle CC. Aerodynamic particle size analysis of aerosols from pressurized metered-dose inhalers: comparison of Andersen 8-stage cascade impactor, next generation pharmaceutical impactor, and model 3321 aerodynamic particle sizer aerosol spectrometer. AAPS PharmSciTech. 2003;4:425–33.
35. Suarez S, Hickey AJ. Drug properties affecting aerosol behavior. Resp Care. 2000;45:652–66.
36. Javed I, Ranjha N, Mahmood K, Kashif S, Rehman M, Usman F. Drug release optimization from microparticles of poly (ε-caprolactone) and hydroxypropyl methylcellulose polymeric blends: formulation and characterization. J Drug Deliv Sci Technol. 2014;24:607–12.
37. Umegawa Y, Matsumori N, Oishi T, Murata M. Amphotericin B covalent dimers with carbonyl-amino linkage: a new probe for investigating ion channel assemblies. Tetrahedron Lett. 2007;48:3393–6.
38. Jung SH, Lim DH, Jung SH, Lee JE, Jeong K-S, Seong H, et al. Amphotericin B-entrapping lipid nanoparticles and their in vitro and in vivo characteristics. Eur J Pharm Sci. 2009;37:313–20.
39. Chavanet P, Clement C, Duong M, Buisson M, D'Athis P, Dumas M, et al. Toxicity and efficacy of conventional amphotericin B deoxycholate versus escalating doses of amphotericin B deoxycholate–fat emulsion in HIV-infected patients with oral candidosis. Clin Microbiol Infec. 1997;3:455–61.
40. Moribe K, Maruyama K, Iwatsuru M. Encapsulation characteristics of nystatin in liposomes: effects of cholesterol and polyethylene glycol derivatives. Int J Pharm. 1999;188:193–202.
41. Hąc-Wydro K, Dynarowicz-Łątka P. Interaction between nystatin and natural membrane lipids in Langmuir monolayers—the role of a phospholipid in the mechanism of polyenes mode of action. Biophys Chem. 2006;123:154–61.
42. Bhamra R, Sa'ad A, Bolcsak LE, Janoff AS, Swenson CE. Behavior of amphotericin B lipid complex in plasma in vitro and in the circulation of rats. Antimicrob Agents Ch. 1997;41:886–92.
43. Javed I, Hussain SZ, Ullah I, Khan I, Ateeq M, Shahnaz G, et al. Synthesis, characterization and evaluation of lecithin-based nanocarriers for the enhanced pharmacological and oral pharmacokinetic profile of amphotericin B. J Mater Chem B. 2015;3:8359–65.
44. Singh R, Lillard JW. Nanoparticle-based targeted drug delivery. Exp Mol Pathol. 2009;86:215–23.
45. Hans M, Lowman A. Biodegradable nanoparticles for drug delivery and targeting. Curr Opin Solid St M. 2002;6:319–27.
46. Mbongo N, Loiseau PM, Billion MA, Robert-Gero M. Mechanism of amphotericin B resistance inLeishmania donovani promastigotes. Antimicrobial Agent Ch. 1998;42:352–7.
47. Kanchan V, Panda AK. Interactions of antigen-loaded polylactide particles with macrophages and their correlation with the immune response. Biomaterials. 2007;28:5344–57.
48. Tomazic-Jezic VJ, Merritt K, Umbreit TH. Significance of the type and the size of biomaterial particles on phagocytosis and tissue distribution. J Biomed Mater Res A. 2001;55:523–9.
49. Foged C, Brodin B, Frokjaer S, Sundblad A. Particle size and surface charge affect particle uptake by human dendritic cells in an in vitro model. Int J Pharm. 2005;298:315–22.